

# Updating Circuit Theory – Cable Characterisation

Ian Darney

## Introduction

The article ‘The Virtual Conductor’ derived a theoretical basis for a circuit model which simulated the coupling between a cable and the environment. This article shows how values can be assigned to the components of that model.

A set of tests is described which measure the characteristics of a 15 metre length of twin-conductor cable. The data is then used to create a model which replicates the response of the hardware. It shows how both antenna-mode radiation and differential-mode radiation can be identified and measured. Full details of the process are provided.

## Test Method

Figure 1 illustrates the setup for measuring the frequency response of the radiated emission. The voltage source is a ten-turn transformer clamped on to one of the conductors, halfway along the cable. Apart from the transformer coupling between cable and test equipment, both conductors of the cable are completely isolated.

A monitor turn on the voltage transformer is connected to channel 1 of the oscilloscope to enable the peak to peak voltage of the source to be measured. The article ‘Updating Circuit Theory - The Voltage Injection Transformer’ provides details of the construction and characterisation of this unit.

A current transformer clamped round the cable is used to monitor the unidirectional flow of current in both conductors. Since there is no ground return conductor, the only place for this current to go is out into the environment. It can be defined as the Antenna-Mode current.

The output of the current transformer is connected to channel 2 of the oscilloscope. The peak-to peak amplitude of this signal provides a measure of the antenna-mode current. The article ‘Updating Circuit Theory - The Current Monitor Transformer’ provides details of the construction and calibration of this unit.

The ratio of output current to input voltage has the dimensions of admittance;  $Y$ . Since the current being measured and the voltage source are located in different circuit loops, it can be designated ‘Transfer Admittance’  $YT$ . Since this value has been derived from test results, it is logical to identify this parameter as  $YTt$ . That is

From Figure 1: 
$$YTt = \frac{I_{out}}{V_{in}} \quad (1)$$

The parameter  $YTt$  is a measure of the radiated emission of the cable. Tests were carried out, over a set of spot frequencies, of the input voltage and output current and the transfer admittance calculated for each frequency.

The current transformer was then unclamped from the cable and clamped round the second conductor as shown by Figure 2. Then a further set of tests provided a record of the admittance  $Y_t$  of the cable over the same range of frequencies.

From Figure 2: 
$$Y_t = \frac{I_{out}}{V_{in}} \quad (2)$$

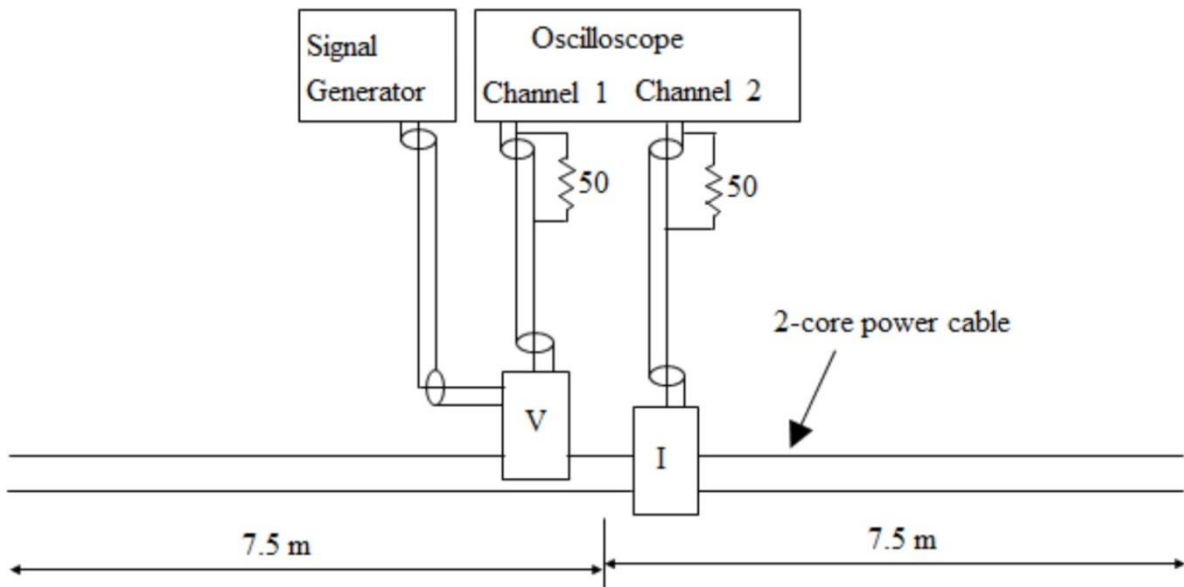


Figure 1 Test to measure emitted radiation characteristics of cable

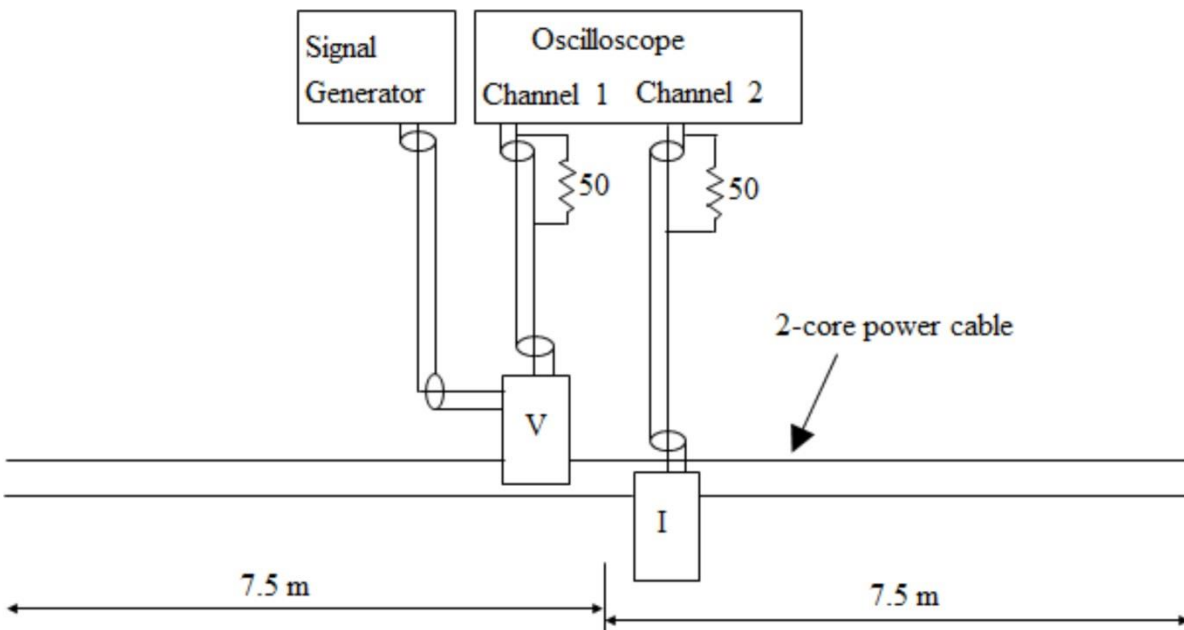


Figure 2 Test setup to measure the cable conductance

## Circuit Modelling

Figure 3 is essentially a copy of the model derived in the article ‘Updating Circuit Theory - The Virtual Conductor’. This model can be transformed into the distributed parameter model by invoking the relationships derived in the article ‘Updating Circuit Theory - Transmission Line Model’.

That is:

$$\begin{aligned} Z_{h_i} &= Z_{o_i} \cdot \tanh\left(\frac{\theta_i}{2}\right) \\ Z_{v_i} &= Z_{o_i} \cdot \operatorname{cosech}(\theta_i) \end{aligned} \quad (3)$$

where

$$\begin{aligned} \theta_i &= \sqrt{(R_{c_i} + j \cdot \omega \cdot L_i) \cdot (G_{c_i} + j \cdot \omega \cdot C_i)} \\ Z_{o_i} &= \sqrt{\frac{R_{c_i} + j \cdot \omega \cdot L_i}{G_{c_i} + j \cdot \omega \cdot C_i}} \end{aligned} \quad (4)$$

## Computations

The computations for this analysis were carried out using Mathcad. This software has the advantages that the equations are presented in the same way as a textbook on mathematics and that all the calculations can be carried out on a single worksheet.

Figure 5 is a copy of the first page of the worksheet. Data from the tests is provided in the form of an array. The parameters  $R1$ ,  $R2$ ,  $R3$ ,  $R4$ ,  $L1$  and  $C1$  on the right hand side are definitions of the components of the circuit model used to calibrate the frequency response of the current transformer. Given a value for the voltage  $V_{ch2}$  at the input of the oscilloscope, it is possible to calculate the amplitude of the current in the secondary winding of this transformer. The current in the primary winding is this secondary current times  $Turns$ , the number of turns on the secondary.

The voltage delivered to the cable under test is also the voltage delivered to a monitor turn on the voltage transformer. Since this monitor turn is in series with a 51 ohm resistor and the load at the input terminals of channel 2 of the oscilloscope is loaded by a 50 ohm resistor, it is easy to calculate the value  $V_{in}$ . The output of the function which processes the data is the vector  $Y_{Tt}$ .

Figure 6 is a copy of the second page of the worksheet. It records the data taken from the setup illustrated by Figure 2 and processes that data in the same way as described above, to create the vector  $Y_t$ .

The third page of the worksheet is illustrated by Figure 7. It first defines the parameters for the lumped-parameter model;  $r11$  and  $r22$  are the radii of the cable conductors;  $r12$  is the separation between the centres of those conductors;  $R_{c1}$ ,  $R_{c2}$ ,  $R_{c3}$ ,  $R_{dm}$ , and  $R_{rad}$  are the resistance values assigned to the components of Figure 3. The parameters  $L_{c1}$ ,  $L_{c2}$  and  $L_{c3}$  are values calculated for the inductors using the equations derived in the article ‘Updating Circuit Theory -The Virtual Conductor’.

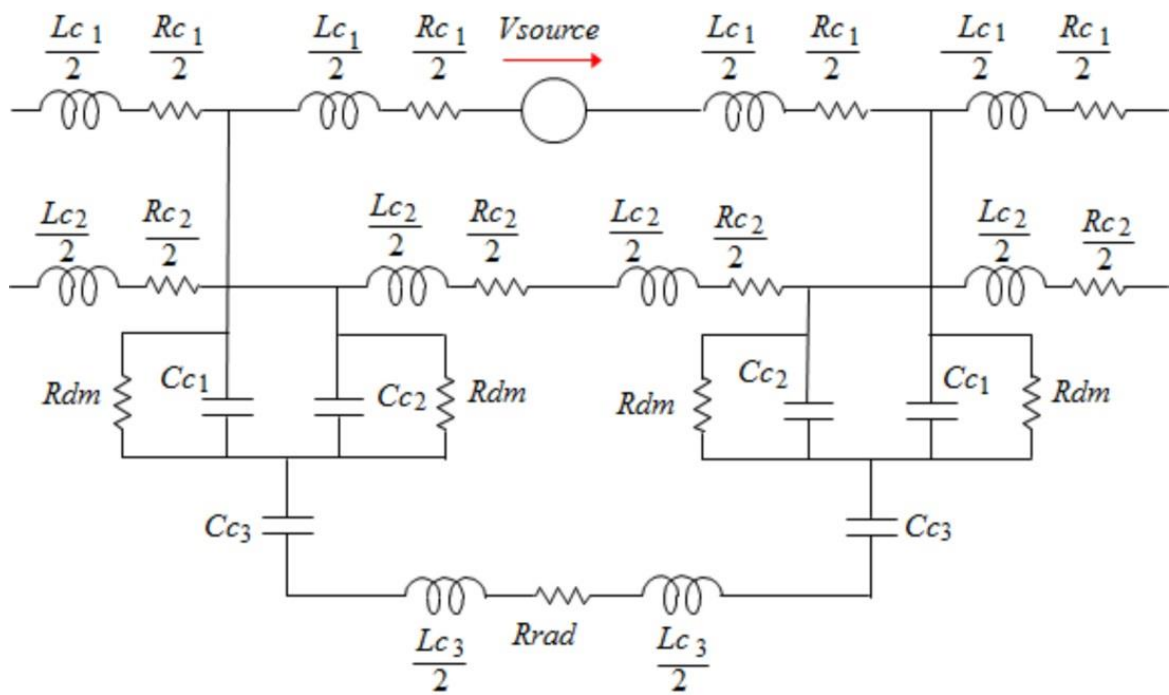


Figure 3 Lumped parameter model

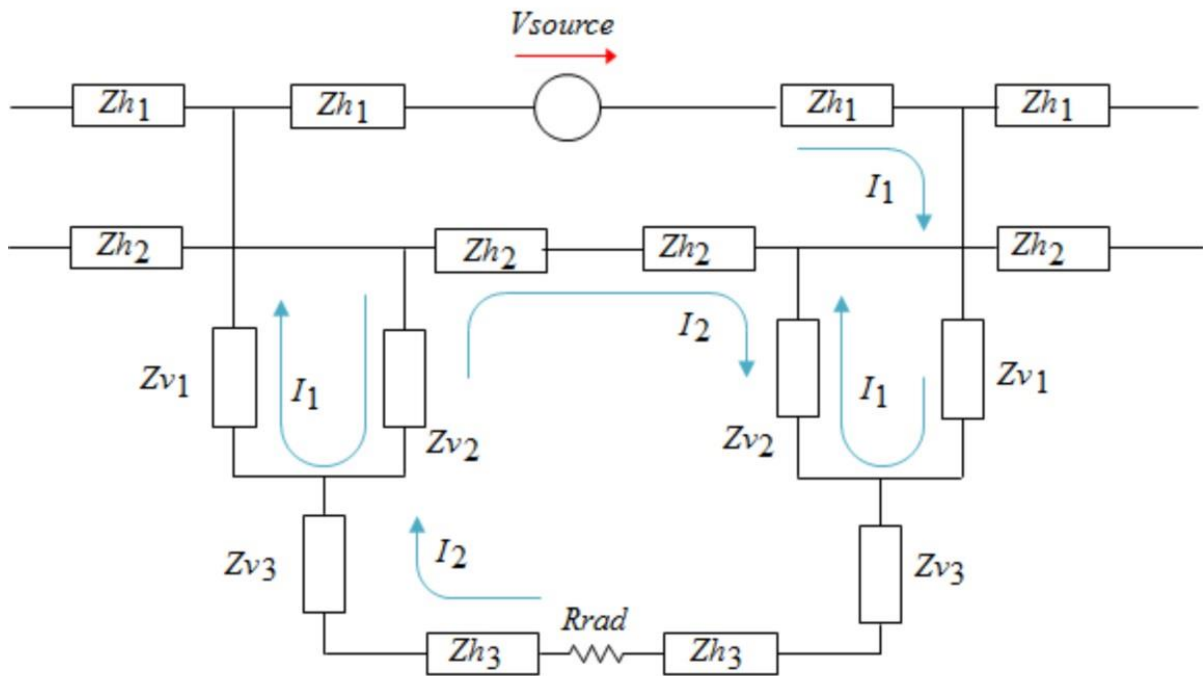


Figure 4 Distributed Parameter model

The values of  $V_{ch2}$  are recorded on the right hand columns of the data arrays on Figures 5 and 6 and  $f_{qa}$  and  $f_{qb}$  are the frequencies at which this voltage reaches a peak value. They are the quarter-wave frequencies where resonance occurs. Since

$$\sqrt{L \cdot C} = T = \frac{4}{fq} \quad (5)$$

then

$$C = \frac{1}{16 \cdot fq^2 \cdot L} \quad (6)$$

The function  $Z_{branch}(f)$  of Figure 7 uses equations (4) and (3) to calculate an impedance value for each branch of Figure 4. The function  $Z_{loop}(f)$  uses these to create an array of loop impedances.  $Z11$  is the sum of the impedances in the loop carrying the current  $I_1$ .  $Z22$  is the sum of the impedances carrying the current  $I_2$ .  $Z12$  is the sum of the impedances carrying both currents. It is negative because they are flowing in opposite directions. The vector  $V$  assigns a voltage of 1 Volt in loop 1 and zero volts in loop 2.

This process has reduced the complexities of the interactions to a pair of simultaneous equations.

$$\begin{aligned} V_1 &= Z11 \cdot I_1 + Z12 \cdot I_2 \\ V_2 &= Z12 \cdot I_1 + Z22 \cdot I_2 \end{aligned} \quad (7)$$

Solving them can be achieved by invoking the built-in function  $lsolve(Z, V)$ . Since this needs to be done over a range of frequencies, the first action at the top of the final page of the worksheet (Figure 8) is to specify  $F_i$  as a set of frequencies between 100 kHz and 20 MHz. The function  $Ym_i$  calculates the values of  $I_1$  and  $I_2$  at each frequency, then creates a vector of values of the magnitude of  $I_1$ , the differential-mode current. The function  $YTm_i$  carries out the same process to create a set of values for  $I_2$ , the antenna-mode current.

There are two plots on each of the graphs on Figure 8. On the upper graph, the first plot is a set of data points defining the transfer admittance  $YTt$ , derived from the test results. The second plot is the response of the transfer admittance  $YTm$ , derived from the response of the model of Figure 4. On the lower graph, the actual admittance  $Yt$  is compared with the simulation  $Ym$ .

That is, the upper graph of Figure 8 compares the response of the setup of Figure 1 with that of the model. The lower graph compares the response of the setup of Figure 2 with that of the model. The same model simulates the response of the cable under review, no matter how it is tested.

This correlation did not happen when the program was run for the first time. Although the shapes of the actual responses were similar to those of the model, there was a significant discrepancy in the amplitude of the peaks.

Data from test on setup of Figure 1

*data1* :=

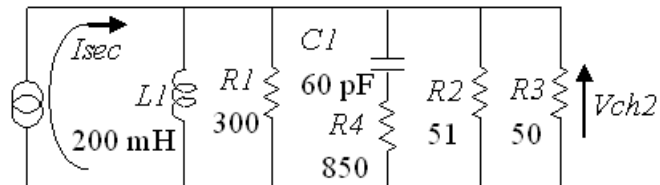
1	420	0.4
2	420	0.4
3	420	0.8
4	420	1.4
5	435	2.4
6	350	3.8
6.5	365	5.8
7	370	11
7.38	370	15
7.5	370	14
7.7	365	11
8	365	7.6
9	365	3.6
10	360	2
11	360	1.8
12	360	1.8
13	360	1.8
14	355	1.6
15	360	1
16	375	2.6
17	320	2
18	270	1
19	280	1
19.8	285	1

column 1: frequency, MHz

column 2: peak-to-peak voltage at channel 1, mV

column 3: peak-to-peak voltage at channel 2, mV

See Figure 7 of the article 'Updating Circuit Theory - The Current Monitor Transformer'.



$$I_{prim} = I_{sec} \cdot Turns$$

$$R1 := 300 \ \Omega$$

$$R2 := 51 \ \Omega$$

$$R3 := 50 \ \Omega$$

$$R4 := 850 \ \Omega$$

$$L1 := 200 \cdot 10^{-6} \ \text{H}$$

$$C1 := 60 \cdot 10^{-12} \ \text{F}$$

$$Turns := 10$$

$$s := 1 .. rows(data1)$$

$$f1_s := data1_{s,1} \cdot 10^6$$

$$YTt_s := \left\{ \begin{array}{l} Vch1 \leftarrow data1_{s,2} \cdot 10^{-3} \\ Vin \leftarrow \frac{51 + 50}{50} \cdot Vch1 \\ Vch2 \leftarrow data1_{s,3} \cdot 10^{-3} \\ \omega \leftarrow 2 \cdot \pi \cdot f1_s \\ Z1 \leftarrow R4 + \frac{1}{j \cdot \omega \cdot C1} \\ Y2 \leftarrow \frac{1}{R1} + \frac{1}{R2} + \frac{1}{R3} + \frac{1}{j \cdot \omega \cdot L1} + \frac{1}{Z1} \\ Isec \leftarrow |Y2| \cdot Vch2 \\ Iprim \leftarrow Isec \cdot Turns \\ Yt \leftarrow \frac{Iprim}{Vin} \end{array} \right.$$

$$Vin \leftarrow \frac{51 + 50}{50} \cdot Vch1$$

$$Vch2 \leftarrow data1_{s,3} \cdot 10^{-3}$$

$$\omega \leftarrow 2 \cdot \pi \cdot f1_s$$

$$Z1 \leftarrow R4 + \frac{1}{j \cdot \omega \cdot C1}$$

$$Y2 \leftarrow \frac{1}{R1} + \frac{1}{R2} + \frac{1}{R3} + \frac{1}{j \cdot \omega \cdot L1} + \frac{1}{Z1}$$

$$Isec \leftarrow |Y2| \cdot Vch2$$

$$Iprim \leftarrow Isec \cdot Turns$$

$$Yt \leftarrow \frac{Iprim}{Vin}$$

Figure 3 Creating a vector of the Transfer Admittance values; *YTt*

Data from tests carried out on setup of Figure 2

$$\begin{array}{l}
 \text{data} := \left( \begin{array}{ccc}
 1 & 420 & 2.8 \\
 2 & 420 & 6.4 \\
 3 & 420 & 11 \\
 4 & 430 & 20.5 \\
 5 & 460 & 60 \\
 5.2 & 480 & 88 \\
 5.5 & 420 & 135 \\
 5.7 & 325 & 110 \\
 6 & 330 & 63.5 \\
 7 & 370 & 25 \\
 8 & 380 & 18.5 \\
 9 & 375 & 5.2 \\
 10 & 375 & 3.6 \\
 11 & 380 & 1.8 \\
 12 & 375 & 0.6 \\
 13 & 380 & 3 \\
 14 & 380 & 6.6 \\
 15 & 390 & 11.5 \\
 15.5 & 405 & 17 \\
 16 & 415 & 26 \\
 16.5 & 395 & 43 \\
 16.8 & 325 & 47 \\
 17 & 280 & 44 \\
 18 & 270 & 20 \\
 19 & 290 & 11.5 \\
 19.8 & 295 & 8.2
 \end{array} \right) \\
 \\
 s := 1..rows(\text{data}) \qquad f_s := \text{data}_{s,1} \cdot 10^6 \\
 \\
 Yt_s := \left\{ \begin{array}{l}
 Vch1 \leftarrow \text{data}_{s,2} \cdot 10^{-3} \\
 Vin \leftarrow \frac{51 + 50}{50} \cdot Vch1 \\
 Vch2 \leftarrow \text{data}_{s,3} \cdot 10^{-3} \\
 \omega \leftarrow 2 \cdot \pi \cdot f_s \\
 Z1 \leftarrow R4 + \frac{1}{j \cdot \omega \cdot C1} \\
 Y2 \leftarrow \frac{1}{R1} + \frac{1}{R2} + \frac{1}{R3} + \frac{1}{j \cdot \omega \cdot L1} + \frac{1}{Z1} \\
 Isec \leftarrow |Y2| \cdot Vch2 \\
 Iprim \leftarrow Isec \cdot Turns \\
 Yt \leftarrow \frac{Iprim}{Vin}
 \end{array} \right.
 \end{array}$$

Figure 6 Creating a vector of the Admittance values  $Yt$ .

$$\begin{aligned}
\mu &:= 4 \cdot \pi \cdot 10^{-7} \\
r11 &:= 0.48 \cdot 10^{-3} & r22 &:= r11 & r12 &:= 1.95 \cdot 10^{-3} & len &:= 7.5 \\
Rc1 &:= 0.02 & Rc2 &:= 0.02 & Rc3 &:= 0 \\
Rdm &:= 350 & Rrad &:= 52 \\
G1 &:= \frac{1}{Rdm} & G2 &:= G1 & G3 &:= 0 \\
Lc1 &:= \frac{\mu \cdot len}{2 \cdot \pi} \cdot \ln\left(\frac{r12}{r11}\right) & Lc2 &:= Lc1 & Lc3 &:= \frac{\mu \cdot len}{2 \cdot \pi} \cdot \ln\left(\frac{len}{r12}\right) \\
fqa &:= 5.66 \cdot 10^6 & fqb &:= 7.55 \cdot 10^6 \\
Cc1 &:= \frac{1}{16 \cdot fqa^2 \cdot Lc1} & Cc2 &:= Cc1 & Cc3 &:= \frac{1}{16 \cdot fqb^2 \cdot Lc3} \\
Zbranch(f) &:= \left| \begin{array}{l} \omega \leftarrow 2 \cdot \pi \cdot f \\ \text{for } k \in 1..3 \\ \quad Gc_k \leftarrow G_k \cdot \frac{f}{fqa} \\ \quad \theta \leftarrow \sqrt{(Rc_k + j \cdot \omega \cdot Lc_k) \cdot (Gc_k + j \cdot \omega \cdot Cc_k)} \\ \quad Zo \leftarrow \sqrt{\frac{Rc_k + j \cdot \omega \cdot Lc_k}{Gc_k + j \cdot \omega \cdot Cc_k}} \\ \quad Zh_k \leftarrow Zo \cdot \tanh\left(\frac{\theta}{2}\right) \\ \quad Zv_k \leftarrow Zo \cdot \operatorname{csch}(\theta) \\ \quad (Zh \ Zv) \end{array} \right. \\
Zloop(f) &:= \left| \begin{array}{l} (Zh \ Zv) \leftarrow Zbranch(f) \\ Z11 \leftarrow 2 \cdot (Zh_1 + Zv_1 + Zh_2 + Zv_2) \\ Z12 \leftarrow -2 \cdot (Zh_2 + Zv_2) \\ Z22 \leftarrow 2 \cdot (Zh_2 + Zv_2 + Zh_3 + Zv_3) + Rrad \\ \left( \begin{array}{cc} Z11 & Z12 \\ Z12 & Z22 \end{array} \right) \end{array} \right. \\
V_{\text{in}} &:= \begin{pmatrix} 1 \\ 0 \end{pmatrix}
\end{aligned}$$

Figure 7 Defining the input parameters and the functions *Zbranch* and *Zloop*

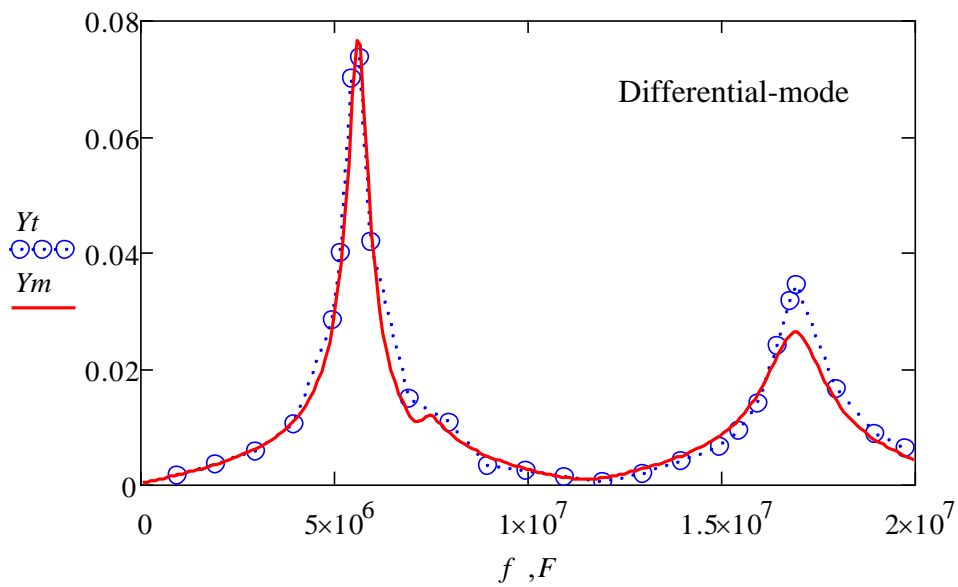
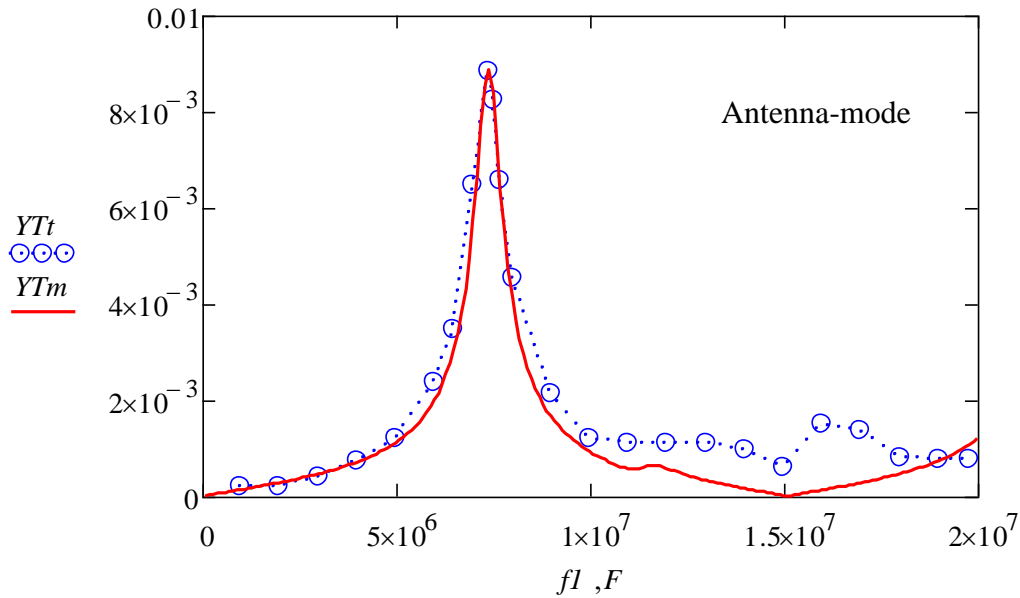


$i := 1..200$

$F_i := i \cdot 10^5$

$YTm_i := \begin{cases} f \leftarrow F_i \\ Z \leftarrow Zloop(f) \\ I \leftarrow lsolve(Z, V) \\ |I_2| \end{cases}$

$Ym_i := \begin{cases} f \leftarrow F_i \\ Z \leftarrow Zloop(f) \\ I \leftarrow lsolve(Z, V) \\ |I_1| \end{cases}$



$Rrad = 52$

$Rdm = 350$

$$\frac{Lc}{2} = \begin{pmatrix} 1.051 \times 10^{-6} \\ 1.051 \times 10^{-6} \\ 6.191 \times 10^{-6} \end{pmatrix} \quad Cc = \begin{pmatrix} 9.278 \times 10^{-10} \\ 9.278 \times 10^{-10} \\ 8.855 \times 10^{-11} \end{pmatrix}$$

Figure 8 Correlating the circuit model with the test data.

By making successive alterations to the value of  $R_{rad}$  between program runs, it was possible to cause the response of the model to coincide with the peak value derived from the results of tests on the configuration of Figure 1. Making successive alterations to the value of  $R_{dm}$  enabled coincidence to occur between the simulation of the model and the results recorded from tests on the configuration of Figure 2.

The results of this process are recorded at the bottom of Figure 8. These include values for the inductors  $L_{c1}$ ,  $L_{c2}$  and  $L_{c3}$ . These values were derived directly from measurements of the radius and separation of the conductors, and from a measurement of the length of the cable. The values calculated for the capacitors  $C_{c1}$ ,  $C_{c2}$  and  $C_{c3}$  were derived from measurements of the frequencies of resonance. The process was similar to that used in successive approximations in solving non-linear equations.

To cater for the fact that the second peak in the response of  $Y_t$  was much smaller than that of the first peak, it was necessary to assume that the resistors  $R_{dm}$  reduced as the frequency increased. This makes sense if it is also assumed that these resistors simulate the radiated current which disappears into the environment. That is, differential mode current departs from both conductors but some of it does not arrive at the other. As the frequency increases, more and more energy is lost. As the frequency reduces, the resistance  $R_{dm}$  increases. Under steady state conditions the resistance of the insulating material of cables is extremely large.

### **Assessment**

The resistance  $R_{rad}$  is a measure of the current departing from the cable when it is acting like a dipole antenna. That is, when the partial current in each conductor is flowing in the same direction. The resistors  $R_{dm}$  are a measure of the differential-mode losses.

The frequency of resonance of the differential-mode current is lower than that of antenna-mode resonance because the dielectric constant of the cable insulation is higher than that of air. So the propagation velocity of the electromagnetic field is reduced.

At frequencies above 10 MHz, resonances occur in each section of the cable due to the discontinuity created by the test equipment at the centre. So the emission is higher than that of the simulation.

It is useful to note that constant values are assigned to the inductors and capacitors in this model, and that the values assigned to resistors vary with frequency.

Since the inductance, capacitance, resistance and admittance of the cable are proportional to length, it is a simple matter to calculate the values which would be assigned to different cable lengths.

### **Conclusion**

A circuit model has been developed which can simulate the coupling between a twin-conductor cable and the environment.